

Supplementary Information for

# Spongy Structure of CdS Nanocrystals Docrated with Dye Molecules for Semiconductor Sensitized Solar Cells

*Tao Ling<sup>†</sup>, Ming-Ke Wu<sup>†</sup>, Kai-Yang Niu, Jing Yang, Zhi-Ming Gao, Jing Sun, Xi-Wen Du\**

School of Materials Science and Engineering, Tianjin University, Tianjin, 300072, P. R.  
China

E-mail: [xwdu@tju.edu.cn](mailto:xwdu@tju.edu.cn)

---

<sup>†</sup> The two authors contribute equally to the present work

## **1. Control the Hole Size of Spongy CdS Nanocrystals**

The morphology of spongy CdS nanocrystals is dependent on the concentration of  $\text{NH}_3\cdot\text{H}_2\text{O}$ . As shown in Figure S1 the porosity and hole size of the as-synthesized spongy CdS nanocrytals increase with the concentration of  $\text{NH}_3\cdot\text{H}_2\text{O}$ . The porosity of spongy structure can influence the performance of S-SSSCs, according to the J-V characterizations (Figure S2), the optimized addition of  $\text{NH}_3\cdot\text{H}_2\text{O}$  is 2 M.

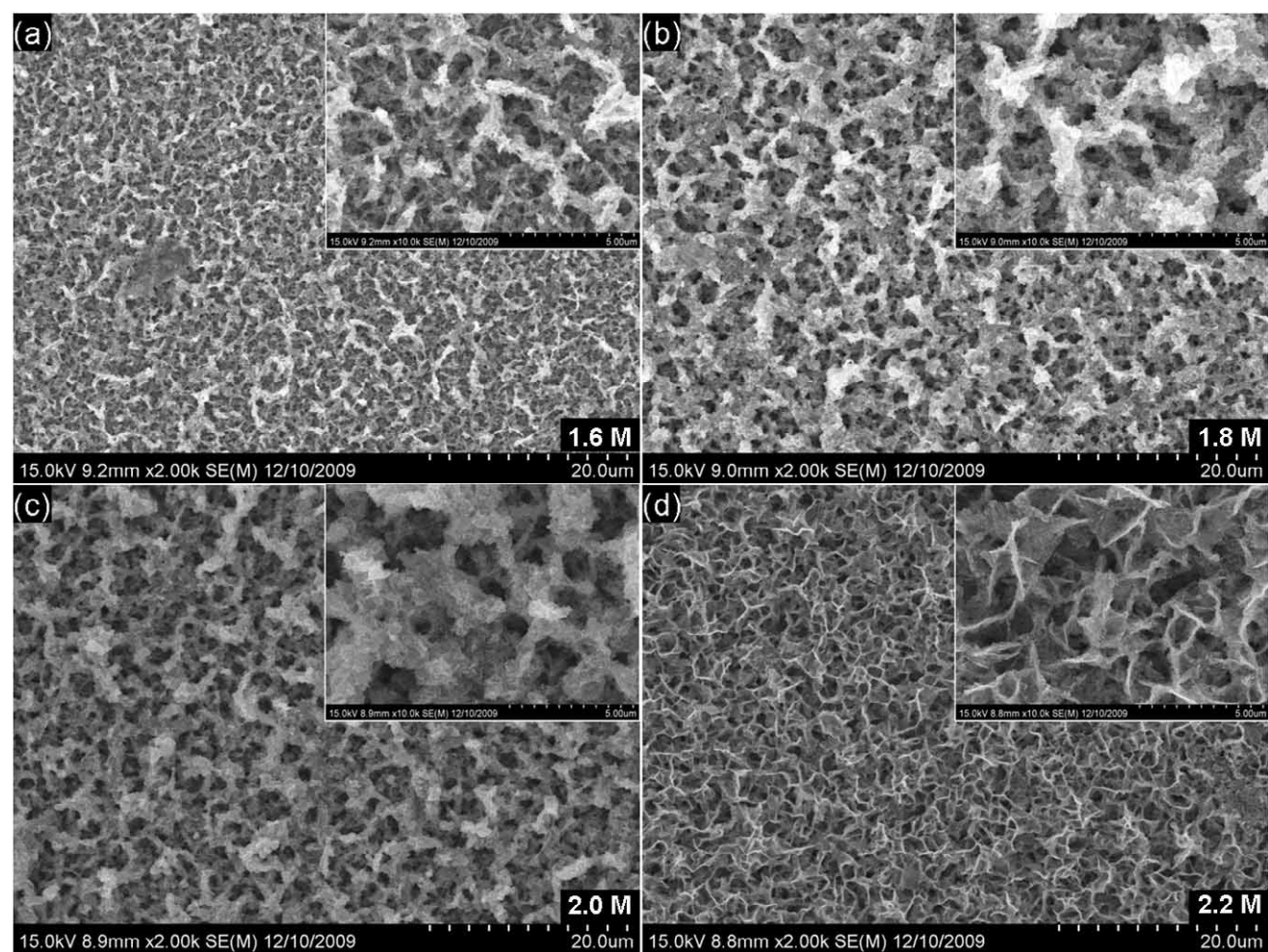


**Figure S1.** SEM images of spongy CdS nanocrystals at different concentration of  $\text{NH}_3\cdot\text{H}_2\text{O}$ .

(a) 1.6 M, (b) 1.8 M, (c) 2.0 M, (d) 2.2 M  $\text{NH}_3\cdot\text{H}_2\text{O}$ .

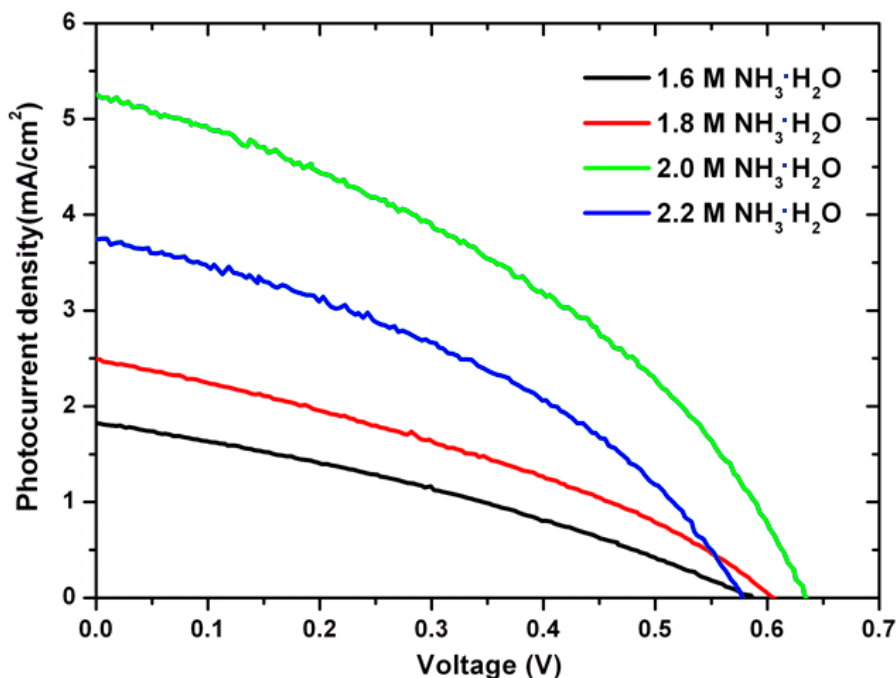


**Figure S2.** J-V characteristics of spongy CdS nanocrystals anodes synthesized at different concentrations of NH<sub>3</sub>·H<sub>2</sub>O.

**Table S1.** Photovoltaic performances of spongy CdS nanocrystals anodes synthesized at different concentrations of NH<sub>3</sub>·H<sub>2</sub>O.

Sample	V <sub>OC</sub> (V)	I <sub>SC</sub> (mA/cm <sup>2</sup> )	FF	η (%)
1.6 M NH <sub>3</sub> ·H <sub>2</sub> O	0.59	1.82	0.33	0.35
1.8 M NH <sub>3</sub> ·H <sub>2</sub> O	0.60	2.49	0.34	0.51
2.0 M NH <sub>3</sub> ·H <sub>2</sub> O	0.63	5.25	0.38	1.27
2.2 M NH <sub>3</sub> ·H <sub>2</sub> O	0.58	3.74	0.39	0.86

## 2. Electrochemical Impedance Spectroscopy (EIS) Analysis

The equivalent circuit used for fitting EIS results was shown in Figure S4a. The impedance of I<sub>3</sub> in electrolyte has been modeled using a finite Warburg element W<sub>s</sub>, and the Pt counter electrode has been described by an RC element R<sub>Pt</sub> and C<sub>Pt</sub>. Similarly, R<sub>FTO</sub> and C<sub>FTO</sub> is from the interface between the exposed FTO and electrolyte. The anode/electrolyte interface is modeled as a transmission line based on a porous electrode that exhibits complex interfacial processes. R<sub>t</sub> is the electron transport resistance of anode, R<sub>ct</sub> is the interfacial charge recombination resistance, and C<sub>μ</sub> is the chemical capacitance.

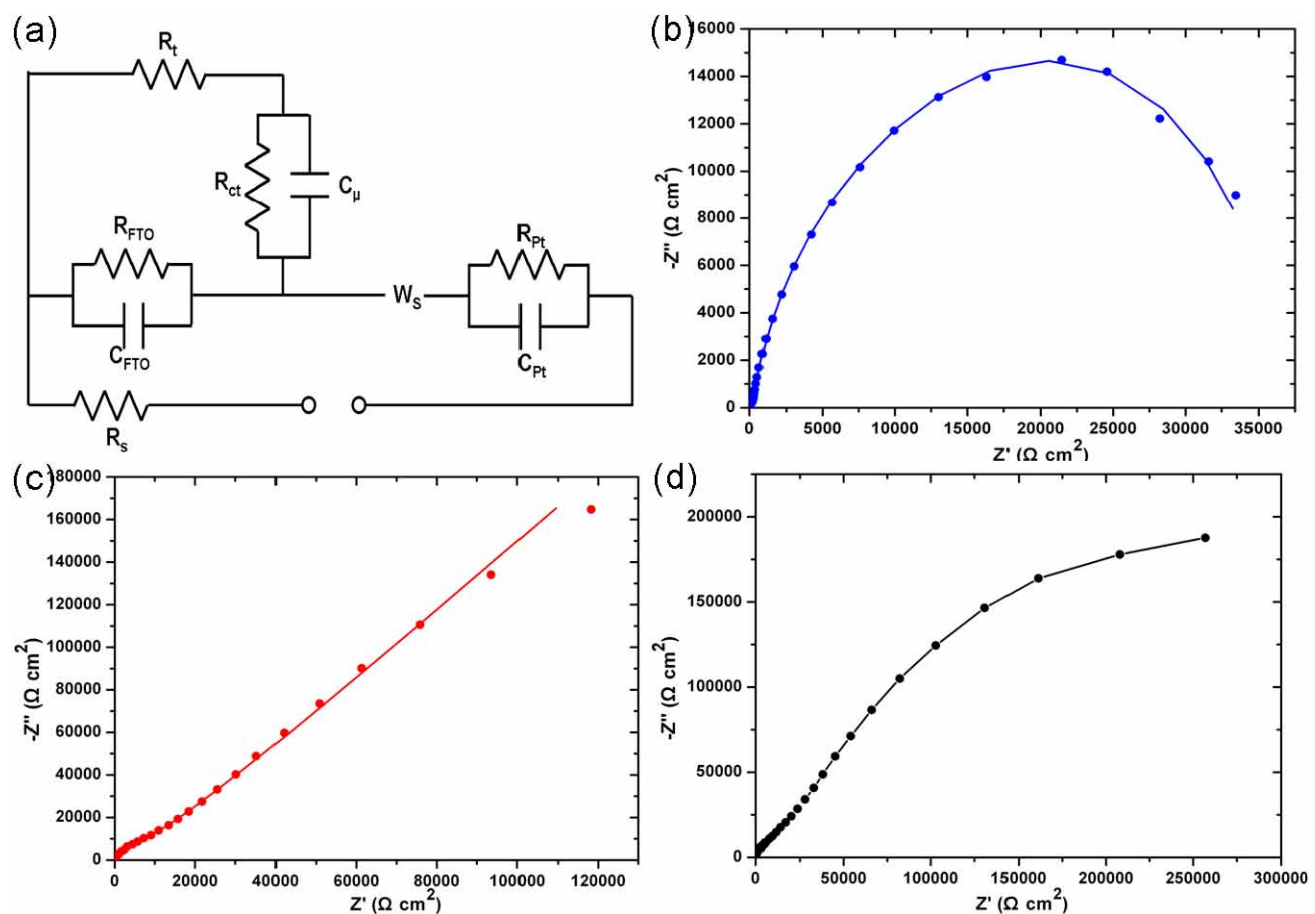


**Figure S3.** EIS analysis on various solar cells. (a) Equivalent circuit of traditional and spongy SSSCs. (b), (c) and (d) are experimental (points) and simulated (lines) EIS results for traditional SSSC, spongy SSSC with N3 dye and spongy SSSC without N3 dye, respectively.

### **3. The Performance of TiO<sub>2</sub> Based solar cells**

In UV-vis absorption spectra (Figure S3a), TiO<sub>2</sub> anodes decorated with N3 dye shows an absorption edge at 700 nm, TiO<sub>2</sub>/CdS has an absorption edge of 512 nm, while the cosensitized TiO<sub>2</sub>/CdS/N3 anode show overlapped absorption features of CdS and N3 dye, the power conversion efficiency of the three type solar cells increase by the sequence of traditional SSSC with TiO<sub>2</sub>/CdS anode, cosensitized SSSC with TiO<sub>2</sub>/CdS/N3 anode, and traditional DSSC with TiO<sub>2</sub>/N3 anode, as listed in Table S2.

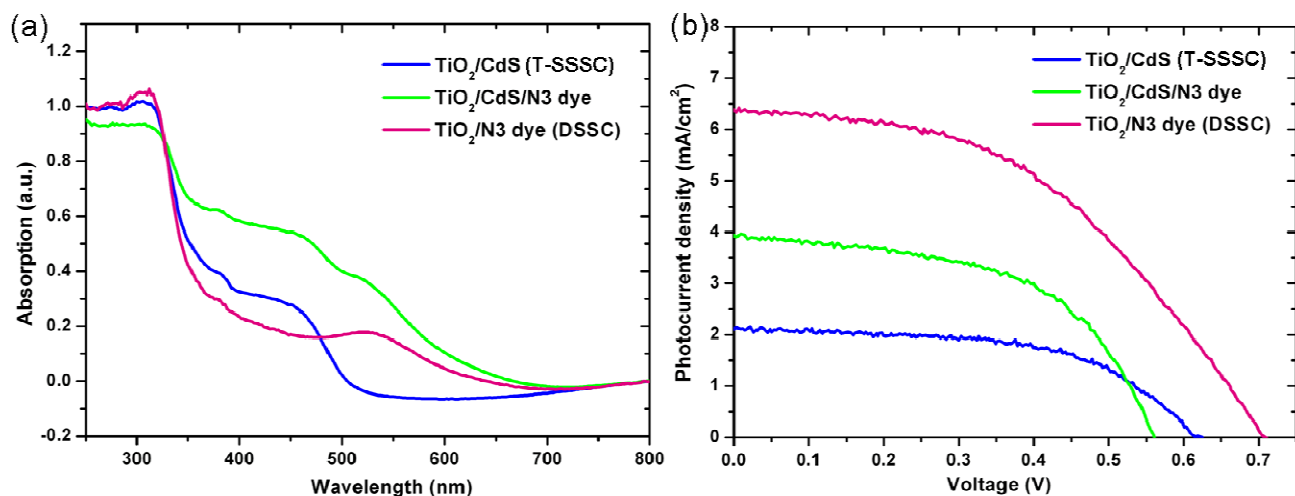


**Figure S4.** The performances of TiO<sub>2</sub> based solar cells. (a) UV-vis absorption spectra and (b) J-V characteristics of TiO<sub>2</sub>/CdS (traditional SSSC), TiO<sub>2</sub>/CdS/N3 dye and TiO<sub>2</sub>/N3 dye (traditional DSSC) systems.

**Table S2.** Photovoltaic performances of TiO<sub>2</sub>/CdS, TiO<sub>2</sub>/CdS/N3 dye and TiO<sub>2</sub>/N3 dye systems

Sample	V <sub>oc</sub> (V)	I <sub>sc</sub> (mA/cm <sup>2</sup> )	FF	η (%)
TiO <sub>2</sub> /CdS	0.61	2.19	0.58	0.77
TiO <sub>2</sub> /CdS/N3	0.56	3.90	0.55	1.20
TiO <sub>2</sub> /N3	0.70	6.33	0.47	2.07

#### 4. The Effect of Annealing on Spongy CdS Anode

Figure S5a shows the XRD patterns of the spongy CdS nanocrystals annealed at different temperatures. Annealing treatments at temperatures higher than 300 °C induce a structural transition in CdS nanocrystals, from cubic to hexagonal structure, and CdSO<sub>3</sub> appears at 500 °C annealing. With respect to peak broadening, we can roughly estimate the crystal size of CdS nanocrystals by  $D = \frac{K_\beta \lambda}{\beta \cos \theta_B}$ .<sup>1</sup> The calculated values of CdS nanocrystals to be 12, 14, 16 and 37 nm for CdS nanocrystals annealed at 120 °C, 300 °C, 400 °C and 500 °C, respectively. The UV-Vis absorption spectra in Figure S5b indicate the absorption increases with the temperature since bigger nanocrystal absorbs more photons.<sup>1</sup> However, the absorption significantly decreases at 500 °C due to the appearance of CdSO<sub>3</sub>.

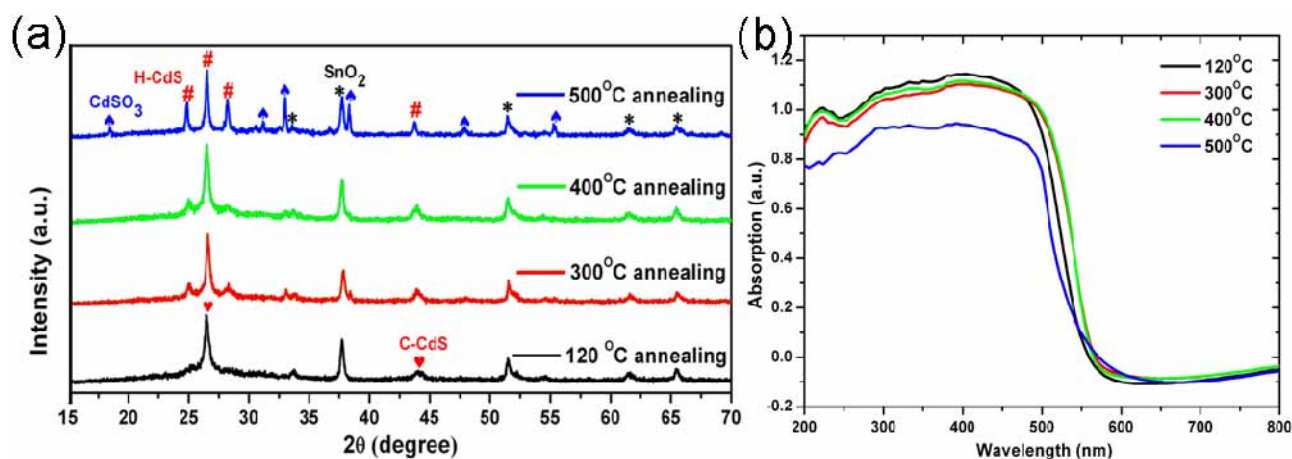


**Figure S5.** The effect of annealing on the crystal structure and absorption property of spongy CdS nanocrystals. (a) XRD patterns and (b) UV–vis absorption spectra of CdS nanocrystals annealed at different temperatures.

#### References

- (1) Tena-Zaera, R.; Katty, A.; Bastide, S.; Lévy-Clément, C. *Chem. Mater.* **2007**, *19*, 1626.